In Situ Interfacial Manipulation of Metastable States Between Nucleation and Decomposition of Single Bismuth Nanoparticle

Chen Luo, Kaihao Yu, Xing Wu,* and Litao Sun*

Nanostructures with rich physical properties are promising for applications in electronics, chemistry, energy and bioscience, etc. The relationship and manipulation among different nanostructures as a hot topic attract many attentions. However, the transformation, such as nucleation events and metastable states, is rarely observed. The electron beam-induced perturbations of the system can be used to manipulate nanostructures by controlling the properties of the focused electron beam. Here, taking advantage of an electron beam to induce the direct growth of bismuth (Bi) nanodroplets on the Bi nanowire, the transformation between nucleation and decomposition processes within the nanoparticles is studied by high-resolution transmission electron microscopy (HRTEM). The results show that the nucleation occurred at the edge of the Bi nanodroplet, and the metastable state in coalesced area introduced the additional interfacial states, determining the nucleation and decomposition of the nanostructure. This study helps to observe the critical process, reduce the gap between theory and experiment for reducing interfacial area to improve the energy storage efficiency.

1. Introduction

The nucleation and the growth of the matters are crucial steps in controlling the size, morphology, growth rate, properties, and reversible transformation in synthesis of materials.[1–6] However, there are still some limitations in understanding the nucleation and decomposition process, especially in phase transitions process.[7] Solidification and liquidation including nucleation and decomposition as first-order phase transitions between liquid and solid are common physical phenomena in our daily life, and have been researched in many fields including material science, physics, chemistry, and biology.[8–11] The traditional understanding of the nucleation and decomposition processing is based on classical nucleation theory. The particle nucleates at a site and then grows outwards by atomic migration and addition. However, the classical nucleation theory is a simplifying assumption, and cannot describe the details of phase transitions, such as the difference in nucleation and growth rate.[3,7,12] Some progresses have been made for further understanding the details of phase transitions including Ostwald's step rule, two step nucleation mechanism and defects/dislocations induced liquidation mechanism.[13–16] Common through all is that these mechanisms introduce an intermediate state − metastable state. The metastable states are found important in nucleation/decomposition phase transitions and should be included in future theoretical investigations.[17] The lack of metastable states make the transitions difficult to predict by theoretical modeling.[12,18] However, some critical processes in the phase transition, such as nucleation events and metastable states, are rarely observed. The experimentally studying becomes the active demand to understand the microscopic mechanisms, especially the metastable states in phase transitions. Nucleation and decomposition are barrier-crossing events, and it is difficult to manipulate and maintain the reversible nucleation/decomposition process.[3] Metastable state is a critical state, the origin and growth of metastable state and how does it affect the phase transition remain a question. The metastable state is hard to be observed when the transitions occur due to the very fast timescale and very small size.[19] The phase transition of colloidal systems is fairly slow, and have been used to study the transition.[20,21] Transmission electron microscopy (TEM) is a powerful tool for the static characterization and dynamic manipulation of nanomaterials at the atomic scale.[22–25] With its high spatial resolution, the atomic structure of metastable states during phase transition in single nanoparticle can be observed clearly. High-energy electron beam in TEM can tailor the structure of the samples by transferring electronic energy to

C. Luo, Prof. X. Wu
Shanghai Key Laboratory of Multidimensional Information Processing
Department of Electronic Engineering
East China Normal University
500, Dongchuan Road, Shanghai 200241, China
E-mail: xwu@ee.ecnu.edu.cn

K. Yu, Prof. L. Sun
SEU-FEI Nano-Pico Center
Key Laboratory of MEMS of Ministry of Education
School of Electronic Science and Engineering
Southeast University
Nanjing 210096, China
E-mail: slt@seu.edu.cn

1800442 (1 of 7)

the samples, which is also known as the electron beam irradiation effects.[26] The electron beam irradiation has been widely used to heat samples, especially for metal nanoparticles.[27,28] Metal nanoparticles with lower melting point and larger surface-to-volume ratio are desirable for electron beam manipulation.[29,30] Some great works have been done to report the process of phase transitions in Bi nanoparticles.[17,28,31–36] There are still some confusions about the metastable states in phase transitions including the origin and growth of metastable state and how does it affect the phase transition. Also the bismuth/bismuth-containing-semiconductor like Bi/BiOCl and Bi/SrBi$_2$Ta$_2$O$_9$ system may induce the extra impurities in studying the intrinsic properties of the phase transition of Bi nanoparticles.[17,28,31,37] In this work, we take advantage of the manipulation ability of electron beam to grow the Bi nanoparticles on the Bi nanowire. The atomic structure and the evolution of the metastable state can be observed clearly by high-resolution TEM (HRTEM). The study shows the whole process about the phase transition of Bi nanoparticles including the nucleation, growth (including coalescence), metastable state process and phase transition. The results show that the nucleation occurred at the edge of the Bi nanodroplet, and the metastable state in coalesced area introduced the additional interfacial states, determining the solidification or liquidation of the nanostructure. The study enables us to explore the complex dynamics during the process of solidification/liquidation transition of Bi

nanoparticles with atomic resolution, which is valuable for understanding the microscopic mechanism of the reversible process driven by metastable states.

2. Results and Discussion

Bismuth nanowires are prepared in AAO template by electrochemical deposition.[38,39] The TEM images of the Bi nanowire sample at the beginning and after irradiation are shown (**Figure 1**). The thickness of the nanowire is uniform (Figure 1a). After irradiation, some Bi nanoparticles grow on a nanowire (Figure 1b). The density of the nanoparticles is about 0.012 nm^{-2}. The detailed morphology of the Bi nanoparticles on a nanowire are shown in the insert (Figure 1b), and the Bi nanoparticles show almost the same spherical morphology. When the sample is irradiated for 2 min, nanoparticles with an average diameter of 5 nm are observed (Figure 1c). The distribution of particle size obeys Gaussian distribution. The diameters of most particles are ranging from 4 to 6 nm. The diameter of nanoparticle is smaller when the nanoparticles close to the carbon film/copper grid due to the high thermal conductivity, and there is almost no particles when the nanowire connect to the carbon film/copper grid (Figure S1, Supporting Information). As the irradiation continues, the particles coalesce, leading to irregularly shaped particles (Figure 1d).

It is particular interesting when we turn our attention back to the nanowire after irradiation. There is something different in
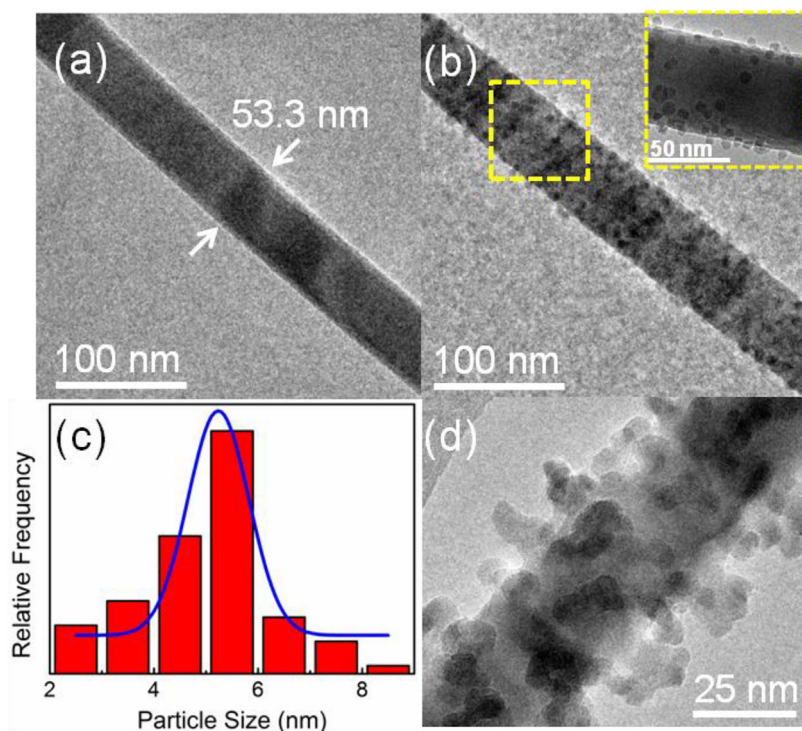
Figure 1. Bi nanowire before and after irradiation. a) Low-magnification TEM image of Bi nanowire before irradiation. The thickness is uniform. b) Low-magnification TEM image of Bi nanowire after 2 min irradiation, the inset shows the higher magnification image of the area highlighted in yellow dashed rectangle. c) The histogram of the distribution of Bi particle size, it follows Gaussian distribution. d) The coalescence of nanoparticles after 10 min irradiation.

interplanar spacing (**Figure 2**). The high resolution transmission electron microscopy (HRTEM) image of the Bi nanowire after irradiation is shown, and the areas which highlighted in red and yellow dashed rectangle are different (Figure 2a). At this time, some Bi nanoparticles can been observed on the nanowire. The lattice fringes at the edge and in the middle of the nanowire show the different interplanar spacing. The interplanar spacing of the areas highlighted in red and yellow dashed rectangle is 0.726 and 0.327 nm, respectively, about two times as long as it (Figure 2b and c). Comparing with corresponding fast Fourier transform (FFT) images (Figure 2b and c), a pair of points which highlighted in green open circle is lost. The lost points represent (202) crystal plane. The (202) crystal plane become blurred gradually and even vanishes at last after irradiation (Figure 2b). The crystal plane corresponding to the crystal plane spacing 0.726 nm cannot be found in the PDF card, and the phenomenon has not been reported before. It may be due to the heat effect induced by irradiation, could be the intermediate state of the liquidation of Bi nanowires. For further studying this phenomenon, the corresponding inverse Fourier transform (IFFT) image is made (Figure 2d and e). Three and four pairs of diffraction point are used as the mask to simulate the IFFT images, respectively. The phenomenon that the increase of crystal plane spacing induced by the vanishing of the diffraction points can be seen clearly.

The nucleation and growth process of the Bi nanoparticle are shown (**Figure 3**). The nanowire is uniform before irradiation (Figure 1a). After irradiation, the nanowire begins to melt and some small liquid droplets appear (Figure S2, Supporting Information). The Bi nanowire is sensitive to electron beam radiation,[40] and the electron beam can create a significant temperature rise in the material due to electron thermal spikes and poor thermal conduction away from the nanowires.[41] The electron beam used as a heater here, which is similar to a simple

heating effect, can induce a reversible phase transitions of Bi nanoparticles.[17,28] According to Fisher's equation,[42] a quantitatively temperature increase on semiconductor can be estimated as:

$$\Delta T = \frac{I}{4\pi ke}\left(\frac{\Delta E}{d}\right)\left(1 + 2\ln\frac{b}{r_0}\right)$$

where ΔT is the maximum temperature rise caused by an electron beam, k is the thermal conductivity, ΔE is the total energy loss per electron in a sample of thickness d, b is the radius of the heat sink which is approximately equal to the radius of Bi wire, and r_0 is the beam radius. Here, $\Delta E/d$ is considered as a constant of $0.5\,\text{eV}\,\text{nm}^{-1}$ at 300 keV, b is taken to be 20 μm, and r_0 is taken to be 27 nm, k is taken to be 0.8 W/m/K which is the thermal conductivity of Bi nanowire of which the thickness is about 50 nm.[43] I is taken to be 270 nA ($40\,\text{A}\,\text{cm}^{-2}$). By using these parameters, ΔT is about 220 K. The thermal conductivity of Bi nanowires is poor, and the heat cannot diffuse quickly during the e-beam irradiation. The melting point of bulk Bi is low and decreases for decreasing dimensions of the nanoparticles. The radius of the nanoparticle shown in Figure 1 is determined to be 6–8 nm, and the melting and freezing temperature of Bi nanoparticles is calculated about 174 and 148 °C, respectively (See Supporting Information). Assuming the effect of the electron beam can be modeled as a simple heating source to manipulate the reversible phase transition of Bi nanoparticles. The simulated images of heat distribution in decomposition and nucleation process are made based on this model by using Comsol Multiphysics and will discuss in the following (Figure S9, Supporting Information).

The nanodroplet shows a uniform contrast, suggesting that it remains in a liquid phase,[44] which is supported by the FFT pattern (Figure S2, Supporting Information). The liquid phase
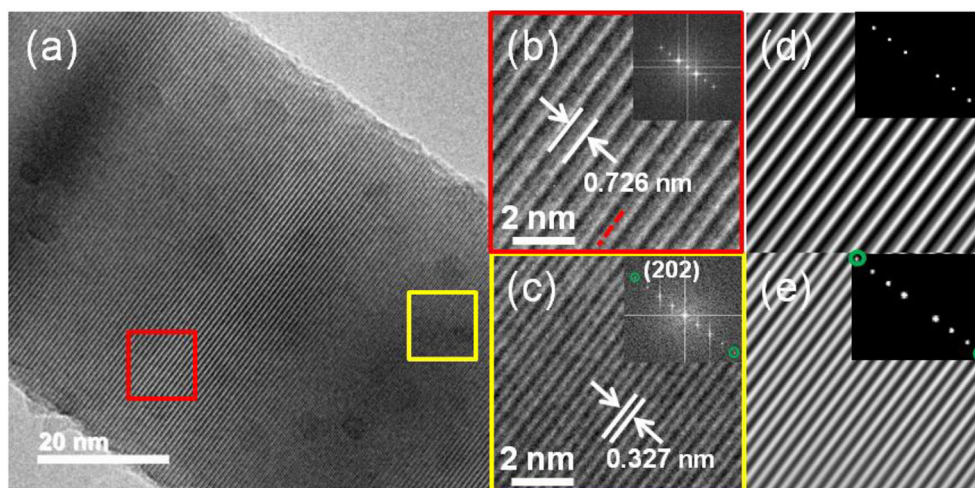
Figure 2. Selected areas with e-beam assisted grown Bi nanoparticles. a) High resolution transmission electron microscopy (HRTEM) image of Bi nanowire after irradiation. b) and c) HRTEM images of the areas highlighted in red and yellow dashed rectangle at higher magnification. The interplanar spacing of the areas highlighted in red and yellow dashed rectangle is 0.726 and 0.327 nm, respectively. Inset shows the corresponding fast Fourier transform (FFT) images, the diffraction points are sharp showing the high quality of the Bi nanowires. d) and e) Corresponding inverse Fourier transform (IFFT) images. Inset shows the mask used to simulate corresponding IFFT image.
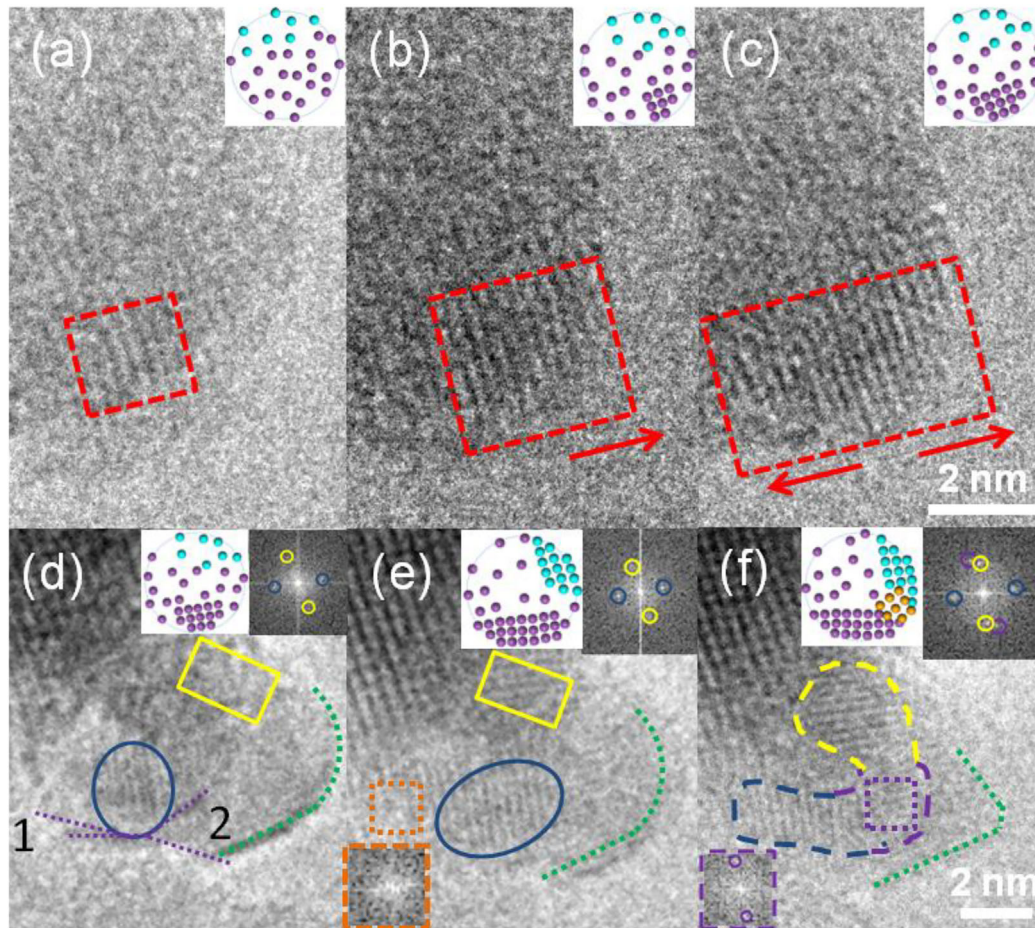
Figure 3. The solidification process of the Bi nanoparticle. a–c) The area highlighted in red dashed rectangle shows the nucleation at edge, red arrow shows the direction of growth process. d–f) Area in blue open circle shows the growth of crystal nucleus. 1 and 2 associated with purple dashed lines in (d) show the different contact angles, approximately 17° and 53°, respectively. Areas in yellow rectangle show nucleation at edge. The crystal orientation is different from the areas in blue open circle. Green dashed line shows the evolution of the profile of nanodroplet. The inset at the bottom left in (e) is the FFT pattern of the area in orange dashed rectangle. The area in purple dashed rectangle in (f) shows the appearance of a new/intermediate phase. The inset at the bottom left in (f) is the FFT pattern of the area in purple dashed rectangle. The inset at the top right in (d–f) shows the FFT pattern of the whole particle at different stages, respectively. The purple, cyan, and yellow balls represent the Bi atoms in grain A, grain B, and metastable states, respectively.

can be confirmed by other methods such as contact-angle hysteresis,[45] and a slip process of the nanostructure is also a characteristic of liquid droplets.[31,45] The nucleation of the nanoparticles starts at the edge of the droplets, and then recrystallize to Bi nanoparticles. Irradiation under the electron beam can cause the charging of materials in TEM due to the Auger electrons,[46] and the build-up of charge can alter the surface energy and then change the melting temperature.[47,48] The electric conductance of Bi nanowire is poor and the charges in nanoparticles cannot flow to nanowire easily, and charges can build up at the interface. These charges can change the surface potential and alters the surface tension, and improve a higher effective melting temperature of Bi nanoparticles. The transformation from liquid droplets to solidification of the Bi nanoparticles occurs due to the improved melting temperature. The density of charges tends to be higher at the edge due to the poorer

electric conductance of between Bi nanoparticles and vacuum than Bi nanoparticles and nanowire. And the melting temperature of Bi nanoparticles is higher at the edge near vacuum. The temperature of the vacuum is lower while the nanowire near the edge of nanoparticles is under heating by electron beam, and the heat can diffuse more easily to the vacuum than nanowire. The colder temperature of vacuum and the poor thermal conductivity of Bi nanowire can cause the nucleation at edge firstly (Figure 3a). The crystal orientation of nanoparticles is random (Figure S3, Supporting Information), and is independent of the orientation of substrate. Once the droplet solidify as the nucleation at edge, the charges build up at the interface between the nucleation area and liquid area due to the higher electric conductance of liquid droplets than solid nucleation area, and improve the melting temperature leading to the growth of nanoparticle. Also, the size dependent melting

point will induce the liquid–solid phase transition. At the initially stage, the formed Bi nanoparticles show liquid phase due to their low melting point under heating by the electron beam. Accompanying with the size large than a critical size, the Bi nanoparticle shows a higher melting points than the equilibrium temperature induced by the electron beam heating. It means the Bi nanodroplet is undercooled, which results in the liquid to solid phase transformation. Then it grows along the edge after several seconds (Figure 3b and c). On the other hand, when the droplet solidifies, the nanodroplet undergoes a shape change from spherical to a faceted morphology leading to different contact angle (Figure 3d). The green dashed line shows the evolution of the profile of nanodroplet from spherical to a faceted morphology (Figure 3d–f). The melting temperature is dependent on the contact angle, it decreases with decreasing contact angle.[49] And the different growth rate can be seen (Figure 3d and e). From the FFT pattern of the orange dashed area (Figure 3e), the quasi-solid nanostructure can be seen, indicating the pre-solidification state. The nucleation at edge and growing along the edge can also been seen in the yellow highlighted area (Figure 3d–f), and the crystal orientation is different from the area highlighted in blue rectangle (Figure S4a, Supporting Information). The result agrees with the simulated images of heat distribution in single Bi nanoparticle under the irradiation, which show that the heat distribution changed severely and nucleate more easily at the edge (Figure S9, Supporting Information). As the two solid areas growing along the edge, they connect to each other and a new/intermediate phase appears in the connected area (Figure 3f). The new/intermediate phase is a metastable state and the area is not stable. The new/intermediate phase increases the entropy of the nanodroplet and will induce the liquidation of the solid area under the following irradiation. The further analysis was made by using polar coordinate transform of the FFT (Figure S6, Supporting Information).[50] The evolution of the crystalline order of different areas in single nanoparticles in different growth stages can be seen clearly, and it will be discussed in detail in the following. It is interesting to find that the thermal contact area between the Bi liquid and the support

before and after crystallization of the nanoparticle is same (Figure S4b and c, Supporting Information), and demonstrating the heat diffuses more easily to the vacuum rather than nanowire.[17]

Figure 4 shows the fluctuation process of the growth of Bi nanoparticle. After nucleation, the nanoparticle grows along the edge. At this time, the nucleation occurs at another point at the edge and grows (Figure 4a). The area in red and blue open circle indicates two growing crystal nucleuses, and the amorphous area in yellow open circle shows that the area remains liquid state. Once the two crystal nucleuses grow and coalesce, the solid area becomes bigger. The spherical nanostructure can be divided into two parts, the bigger solid area and the smaller liquid area. The melting temperature of Bi is dependent on the dimensions of Bi materials. The bigger solid area has higher melting temperature, and more stable of the grow process. However, the coalesced area is polycrystalline or amorphous, the interface can be seen clearly (Figure 4a and S5, Supporting Information). This area is metastable and easy to melt under irradiation (Figure 4b), and the defects can also induce the liquidation process.[17] The fluctuation of nucleation and liquidation process goes until the coalesced area is stable enough under the irradiation. In our case, one of the phases disappears in the particle and the stable coalesced area is single crystal (Figure 4c and S7, Supporting Information), and then the nanodroplet transforms into nanoparticle.

The transformation between solid and liquid can be quantified by calculating the crystalline order of the entire nanoparticle, and the crystalline order of the nanoparticle can be determined from the FFT patterns of TEM images.[17] Using this method, the process of the liquidation and solidification can be explored quantitatively (**Figure 5**, S6–S8, Supporting Information). The crystal nucleus grows uniformly before the coalescence happens (Figure 3a-c and 5). At the beginning of two areas connecting to each other, the growth rates of the two areas decrease but the whole growth rates of nanoparticle remain the same. It is induced by the formation of the new/intermediate phase (Figure 5). The whole nanoparticle is still in the solidification process, and a new/intermediate phase appears at this time. When the new/intermediate phase appears in single
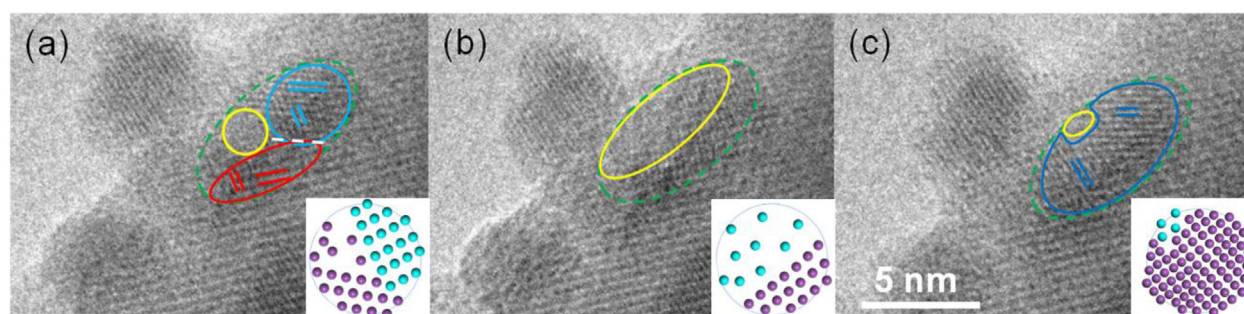
Figure 4. Fluctuation process of the growth of Bi nanoparticle. a–c) Area highlighted in green dashed open circle shows one nanodroplet. Area highlighted in yellow open circle shows the amorphous area. Area highlighted in blue open circle shows one solid area, and area highlighted in red open circle shows another solid area. The white dashed line shows the interface in coalesced area. Area highlighted in dark blue open circle shows the area after coalescence event. The red, blue, and dark blue lines show the crystal orientation. The purple and cyan balls represent the Bi atoms in grain A and grain B, respectively.
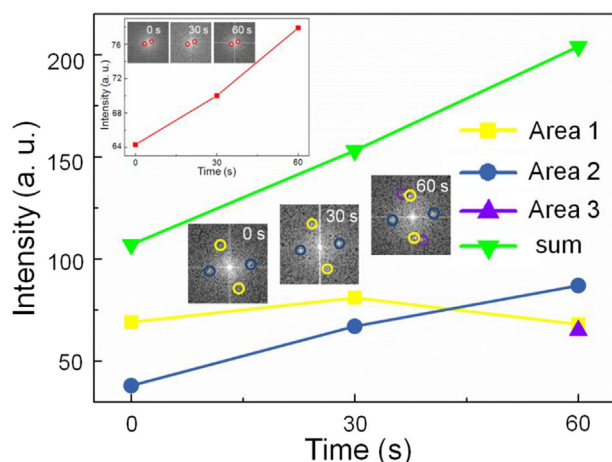
Figure 5. Quantifying the solidification processing of the nanoparticle. The inset at the top left is the peak intensity of the Fourier spectrum as a function of time, showing the growth rate of crystal nucleus is uniform before they connected to each other. The FFT patterns correspond to Figure 3a–c, respectively. The inset in the middle is the FFT patterns corresponding to Figure 3d–f, respectively. The diffraction points corresponding to the same region share the same color, and the green points indicate the whole intensity of the nanoparticle. At 60 s, a new/intermediate phase highlighted in purple circle appears, and is a critical point in phase transitions.

nanoparticle, the nanoparticle is in a metastable state, and tends to liquefy (Figure 3, 5, and S6, Supporting Information). When the phases reduce in single nanoparticle, the nanoparticle tend to solidify (Figure 4, S7 and S8, Supporting Information). The new/intermediate phase also appears in another Bi nanoparticle and leading to the liquidation process (Figure 4, S7 and S8, Supporting Information). The new/intermediate phase as a metastable state appears at the coalesced area introducing the additional interfacial states (Figure 4a and S5, Supporting Information).

3. Conclusions

The whole fluctuation process of Bi nanodroplet under electron beam irradiation can be described as follows: At first, nucleation occurs at the edge due to the aggregation of charges and the diffusion of temperature. The charges build up around the nucleation area when the nucleation occurs, leading to a uniform growth of the crystal nucleus. The nucleation occurs at another point at the edge and grows. Then crystal nucleuses grow and coalesce, a faceted morphology can be seen at this time. Once the coalesced area is not single crystal and melts under irradiation, one solid area can be divided into several small solid areas with lower melting temperature due to the smaller size. Then the small solid area becomes smaller until it disappears or enters next cycle.

Supporting Information

Supporting Information is available from the Wiley Online Library or from the author.

[1] K. L. Sowers, B. Swartz, T. D. Krauss, *Chem. Mater.* **2013**, *25*, 1351.
[2] S. G. Kwon, T. Hyeon, *Small* **2011**, *7*, 2685.
[3] D. W. Oxtoby, *Acc. Chem. Res.* **1998**, *31*, 91.
[4] X. Peng, *Nano Res.* **2009**, *2*, 425.
[5] J. Park, J. Joo, S. G. Kwon, Y. Jang, T. Hyeon, *Angew. Chem. Int. Edit.* **2007**, *46*, 4630.
[6] C. Zhu, F. Xu, H. Min, Y. Huang, W. Xia, Y. Wang, Q. Xu, P. Gao, L. Sun, *Adv. Funct. Mater.* **2017**, *27*, 1606163.
[7] A. Samanta, M. E. Tuckerman, T.-Q. Yu, E. Weinan, *Science* **2014**, *346*, 729.
[8] O. G. Shpyrko, R. Streitel, V. S. K. Balagurusamy, A. Y. Grigoriev, M. Deutsch, B. M. Ocko, M. Meron, B. Lin, P. S. Pershan, *Science* **2006**, *313*, 77.
[9] A. Tabazadeh, Y. S. Djikaev, H. Reiss, *Proc. Natl. Acad. Sci. USA* **2002**, *99*, 15873.
[10] L. C. Jacobson, V. Molinero, *J. Am. Chem. Soc.* **2011**, *133*, 6458.
[11] P. G. Vekilov, *Cryst. Growth Des.* **2010**, *10*, 5007.
[12] P. G. Vekilov, *Nat. Mater.* **2012**, *11*, 838.
[13] P. R. ten Wolde, D. Frenkel, *Science* **1997**, *277*, 1975.
[14] A. M. Alsayed, M. F. Islam, J. Zhang, P. J. Collings, A. G. Yodh, *Science* **2005**, *309*, 1207.
[15] W. Ostwald, *Z. Phys. Chem.* **1897**, *22*, 289.
[16] S. Y. Chung, Y. M. Kim, J. G. Kim, Y. J. Kim, *Nat. Phys.* **2009**, *5*, 68.
[17] Y. Li, L. Zang, D. L. Jacobs, J. Zhao, X. Yue, C. Wang, *Nat. Commun.* **2017**, *8*, 14462.
[18] V. J. Anderson, H. N. Lekkerkerker, *Nature* **2002**, *416*, 811.
[19] Z. Wang, F. Wang, Y. Peng, Z. Zheng, Y. Han, *Science* **2012**, *338*, 87.
[20] E. Sanz, C. Valeriani, D. Frenkel, M. Dijkstra, *Phys. Rev. Lett.* **2007**, *99*, 055501.
[21] Z. Wang, F. Wang, Y. Peng, Y. Han, *Nat. Commun.* **2015**, *6*, 6942.
[22] X. Wu, C. Luo, P. Hao, T. Sun, R. Wang, C. Wang, Z. Hu, Y. Li, J. Zhang, G. Bersuker, L. Sun, K. Pey, *Adv. Mater.* **2018**, *30*, 1703025.
[23] X. Liu, T. Xu, X. Wu, Z. Zhang, J. Yu, H. Qiu, J. H. Hong, C.-H. Jin, J. X. Li, X. R. Wang, *Nat. Commun.* **2013**, *4*, 1776.
[24] X. Wu, D. Cha, M. Bosman, N. Raghavan, D. B. Migas, V. E. Borisenko, X. X. Zhang, K. Li, K. L. Pey, *J. Appl. Phys.* **2013**, *113*, 114503.
[25] X. Wu, D. Migas, X. Li, M. Bosman, N. Raghavan, V. Borisenko, K. Pey, *Appl. Phys. Lett.* **2010**, *96*, 172901.

[26] C. Luo, C. Wang, X. Wu, J. Zhang, J. Chu, *Small* **2017**, *13*, 1604259.

[27] S. Wu, Y. Jiang, L. Hu, J. Sun, P. Wan, L. Sun, *Nanoscale* **2016**, *8*, 12282.

[28] J. B. Wagner, M. G. Willinger, J. O. Müller, D. S. Su, R. Schlögl, *Small* **2006**, *2*, 230.

[29] K. Y. Niu, J. Park, H. Zheng, A. P. Alivisatos, *Nano Lett.* **2013**, *13*, 5715.

[30] T. J. Park, G. C. Papaefthymiou, A. J. Viescas, A. R. Moodenbaugh, S. S. Wong, *Nano Lett.* **2007**, *7*, 766.

[31] Y. Li, B. R. Bunes, L. Zang, J. Zhao, Y. Li, Y. Zhu, C. Wang, *ACS Nano* **2016**, *10*, 2386.

[32] J. Li, J. Chen, H. Wang, N. Chen, Z. Wang, L. Guo, F. L. Deepak, *Adv. Sci.* **2018**, *5*, 1700992.

[33] J. Li, Z. Wang, F. L. Deepak, *J. Phys. Chem. Lett.* **2018**, *9*, 961.

[34] J. Li, Z. Wang, F. L. Deepak, *ACS Nano* **2017**, *11*, 5590.

[35] J. Li, Q. Li, Z. Wang, F. L. Deepak, *Cryst. Growth Des.* **2016**, *16*, 7256.

[36] Y. Li, M. Huang, L. Zang, D. L. Jacobs, J. Zhao, Y. Zhu, C. Wang, *Cryst. Growth Des.* **2018**, *18*, 5808.

[37] X. Chang, S. Wang, Q. Qi, M. A. Gondal, S. G. Rashid, S. Gao, D. Yang, K. Shen, Q. Xu, P. Wang, *Dalton Trans.* **2015**, *44*, 15888.

[38] Y. Xia, J. A. Rogers, K. E. Paul, G. M. Whitesides, *Chem. Rev.* **1999**, *99*, 1823.

[39] C. R. Martin, *Chem. Mater.* **1996**, *8*, 1739.

[40] Y. Gao, H. Niu, C. Zeng, Q. Chen, *Chem. Phys. Lett.* **2003**, *367*, 141.

[41] T. Yokota, M. Murayama, J. M. Howe, *Phys. Rev. Lett.* **2003**, *91*, 265504.

[42] S. Fisher, *Radiat. Eff.* **1970**, *5*, 239.

[43] A. L. Moore, M. T. Pettes, F. Zhou, L. Shi, *J. Appl. Phys.* **2009**, *106*, 034310.

[44] J.-G. Lee, H. Mori, H. Yasuda, *J. Mater. Res.* **2005**, *20*, 1708.

[45] U. M. Mirsaidov, H. Zheng, D. Bhattacharya, Y. Casana, P. Matsudaira, *Proc. Natl, Acad. Sci. USA* **2012**, *109*, 7187.

[46] J. Cazaux, *Ultramicroscopy* **1995**, *60*, 411.

[47] J. G. Che, C. T. Chan, *Phys. Rev. B* **2003**, *67*, 125411.

[48] A. Y. Lozovoi, A. Alavi, *Phys. Rev. B* **2003**, *68*, 245416.

[49] V. B. Storozhev, *Surf. Sci.* **1998**, *397*, 170.

[50] Y. Fan, A. W. Robertson, Y. Zhou, Q. Chen, X. Zhang, N. D. Browning, H. Zheng, M. H. Rummeli, J. H. Warner, *ACS Nano* **2017**, *11*, 9435.